High Extinction Ratio and Large Bandwidth PCF Polarization Filter With Gold-Wires Coated by Monocrystalline Silicon

Zhihua Yu, Zhizhao Jin, Tao Lv, and Li Liu

***Abstract*—A kind of high extinction ratio (ER) and large bandwidth photonic crystal fiber (PCF) polarization filter based on surface plasmon resonance is proposed. The SPP modes can be inspired by two gold-wires to improve the filter characteristics and the effect of surface plasmon resonance is further enhanced by cladding monocrystalline silicon surrounding gold-wires. An asymmetric structure of leakage channel is introduced in y-pol direction axis which intensifies the energy leakage to external cladding, high polarization extinction ratio is occurred. By using the finite element method (FEM), the structural parameters and optical properties are quantitatively analyzed. Numerical analysis shows that two main adjacent resonance peaks appear in y-pol direction, confinement losses of y-pol core mode at the resonance wavelength of 1519 and 1664 nm are 573.33 and 543.21 dB/cm, while the losses of x-pol core mode are 16.97 and 0.98 dB/cm. When the fiber length L=3 mm, the maximum ER reaches 1449 dB at the wavelength of 1519 nm, and the bandwidth with ER better than 20 dB reaches 405 nm. Hence the proposed PCF with gold-wires coated by monocrystalline silicon would have a widely application in optical fiber communication, optical information processing and other fields.**

***Index Terms*—Photonic crystal fiber, polarization filter, surface plasmon resonance, monocrystalline silicon.**

I. Introduction

PHOTONIC crystal fiber (PCF) refers to a fiber with a two-dimensional periodic refractive index structure, which has many peculiar optical characteristics: controllable nonlinearity, endless single mode and adjustable singular dispersion large mode fields. Therefore, the PCF based devices have a significant application in the field of optical communication and sensing. In addition, the development of new technology allows researchers to combine new materials with PCF, such as filling liquid crystals in optical fibers, introducing metal wires into optical fibers, etc. When the surface plasmon resonance (SPR) occurs, metal has a strong absorption effect on incident light. Based on the light absorption capacity, many SPR devices have been designed and studied.

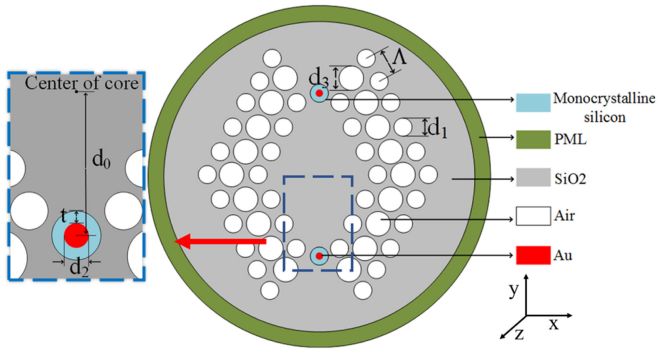

Fig. 1. Cross-section of proposed PCF polarization filter.

Researchers have used various methods to improve the performance of the PCF polarization filter, and the PCF-SPR polarization filter has been proposed. By coating gold film on the air hole, Wang et al. [1] studied a side-leakage PCF filter, the loss of y-pol at wavelength of 1590 nm reaches 1097.94 dB/cm, which is much higher than the x-pol loss of 2.10 dB/cm. Wu et al. [2] reported an elliptical air hole PCF based on SPR, the loss of y-pol is 333.84 dB/cm, which is higher compared to the loss of x-pol of 1.5 dB/cm at the wavelength of 1550 nm. Chang et al. [3] simulated a broadband PCF by coated thin gold film in the air holes. The max extinction ratio of 326 dB is obtained when fiber length is 1 mm. Kawsar Ahmed et al. [4] designed a novel PCF filter with gold coated air holes which has lofty ER and low insertion loss less than 0.06 dB. In 2018, a kind of slotted core PCF was proposed and a low confinement loss with high order nonlinearity was obtained [5]. Researches on the improvement of the air hole arrangement is also underway, in 2020, Lu et al. [6] firstly proposed single-polarization single-mode (SPSM) PCF with uniformly sized air holes, the optimized sample is designed to offer an SPSM band with width of 120 nm. In recent research [7], a broadband panda-like silicon core PCF was studied, the applicable operating wavelength region can reach 1522 nm with the fiber length of 1 mm.

Manuscript received 23 May 2022; revised 24 June 2022; accepted 20 July 2022. Date of publication 25 July 2022; date of current version 5 August 2022. This work was supported in part by the National Natural Science Foundation of China under Grant 62175220, in part by the State Key Laboratory of Advanced Optical Communication Systems and Networks, China, under Grant 2022GZKF018, and in part by the Opening Project of Key Laboratory of Microelectronic Devices and Integrated Technology, Institute of Microelectronics, Chinese Academy of Sciences. *(Corresponding author: Li Liu.)*

The authors are with the School of Automation, China University of Geosciences, Wuhan 430074, China, with the Hubei Key Laboratory of Advanced Control and Intelligent Automation for Complex Systems, Wuhan 430074, China, and also with the Engineering Research Center of Intelligent Technology for Geo-Exploration, Ministry of Education, Wuhan 430074, China (e-mail: yuzhihua@cug.edu.cn; jinzhizhao@cug.edu.cn; lvtaohn@126.com; liliu@cug.edu.cn).

Digital Object Identifier 10.1109/JPHOT.2022.3193395

The common point of the above studies is that there is only one resonant peak within the operating wavelength, and the extinction ratio presents the characteristics of high in the middle and low on both sides. The effect of SPR is highly sensitive to incident light angle θ and the refractive index of dielectric surrounding the metal, researches show that the SPR resonance intensity increases with the increase of the external refractive index, and the resonance peak is red-shifted [8], [9]. Inspired by that, this research proposes for the first time to add a monocrystal silicon layer around the nanowires to stimulate and enhance the SPR effect. Results show that the confinement loss of y-pol at the two main resonance peaks are 573.33 dB/cm and 543.21 dB/cm, respectively, while the losses in the x-pol are both lower than 20 dB/cm, a main operable bandwidth of 405 nm is obtained. Especially, the proposed PCF filter has better filtering performance and larger working bandwidth in 1.55 μm communication band.

II. Stucture Design of PCF Polarization Filter

According to perormance requirements, an asymmetric structure is proposed, and Fig. 1 depicts the structure diagram of the designed PCF. The entire structure contains three layers of air holes which are arranged in triangular lattice with a fixed lattice pitch Λ=1.5 μm, air holes diameter is denoted by d_1 which is optimized to 1 μm in the first and third layers, and the second layer selects air holes with d_3 optimized to 1.36 μm, this arrangement forms two leakage channels on y-axis. In order to excite the surface plasmon, two gold wires with diameter d_2 are placed on y-axis, the initial distance between gold wires and fiber center is set to d_0=4.2 μm. Monocrystalline silicon cladding layers of thickness t are plated on the outside of the gold wires to enhance SPR effect and improve filtering performance. The advanced fiber manufacturing technology provides for the fabrication of the proposed PCF, and a series of production processes can follow the following steps. Firstly, the all-air holes fiber could be fabricated with the help of sol-gel technique [10]. Then by using magnesium thermal reduction reaction to prepare monocrystalline silicon layer, and the chemical vapor deposition technique is employed to deposit reduced silicon nanocrystal on prefabricated gold wires. Finally, the complete microstructure fiber will be produced by embedding coated gold wires into air holes.

In addition, using finer mesh analysis,there are total consisted of 12,696 domain elements and 1,420 boundary elements and a total number of degree freedom solved for 85,841. The convergence error of proposed PCF is 1.7 $\times$ 10^{-9} at wavelength of 1.5 μm. The PML boundary plays a significant role by diminishing undesirable nonphysical electromagnetic radiations. Considering the accuracy and convergence of simulation, the width of PML in this study is optimized to 10% of the cladding diameter.

The dielectric parameters of two gold wires can be defined by Drude equation [11]:

$$\varepsilon_{Au}(\omega) = \varepsilon_1 + i\varepsilon_2 = \varepsilon_\infty - \frac{\omega_p^2}{\omega(\omega + i\omega_c)} \tag{1}$$

TABLE I
Coefficients of Silica and Monocrystalline Silicon

	Silica	monocrystalline silicon
A_1	0.6961663	10.6684293
A_2	0.4079426	0.0030434748
A_3	0.8974794	1.54133408
B_1	$4.67914826 \times 10^{-3}\mu m^2$	$9.091219073 \times 10^{-2}\mu m^2$
B_2	$1.35120631 \times 10^{-2}\mu m^2$	$1.287660172\ \mu m^2$
B_3	$97.9340025\mu m^2$	$1.218816 \times 10^{6}\mu m^2$

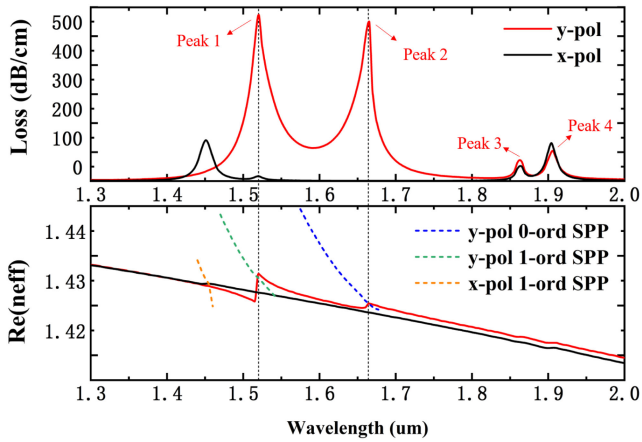

Fig. 2. The confinement loss spectrum and refractive index curve of core mode with parameter of d_0=4.2 μm, d_1=1 μm, d_2=0.4 μm, d_3=1.36 μm, t=0.24 μm.

where ε_∞=9.84 is the dielectric constant of Au, ω=1.36$\times$10^{16}rad/s is the plasma angular frequency, and ω_c=1.45$\times$10^{14}rad/s is the damping frequency.

The dispersion property of silica and monocrystalline silicon can be described by the Sellmeier equation [12]:

$$n^2(\lambda) = 1 + \frac{A_1\lambda^2}{\lambda^2 - B_1} + \frac{A_2\lambda^2}{\lambda^2 - B_2} + \frac{A_3\lambda^2}{\lambda^2 - B_3} \tag{2}$$

where λ is the wavelength of incident light. The Sellmeier coefficients of silica and monocrystalline silicon are given by TABLE I [13]:

The mode confinement loss (CL) is one of the most important parameters of a polarization filter which can be characterized by using the following formula [14]:

$$\alpha_{loss}(dB/cm) = 8.686 \times \frac{2\pi}{\lambda} Im(n_{eff}) \times 10^4 \tag{3}$$

III. Results and Performance Analysis

The geometric parameters stricly determine the performance of fiber polarization filters, in order to better study the dispersion relation of proposed PCF, an original structure is set to d_0= 4.2 μm, d_1=1 μm, d_2= 0.4 μm, d_3=1.36 μm, t = 0.24 μm. Fig. 2 reveals the CL curves of x-pol and y-pol mode, and the effect refractive index curves of core mode and SPP mode with different polarization direction. The red solid line in loss curve represents the confinement loss of y-pol mode, as the wavelength increasing from 1.3 μm, peak 1 and peak 2 was appeared at wavelength of 1519 and 1664 nm. It can be found

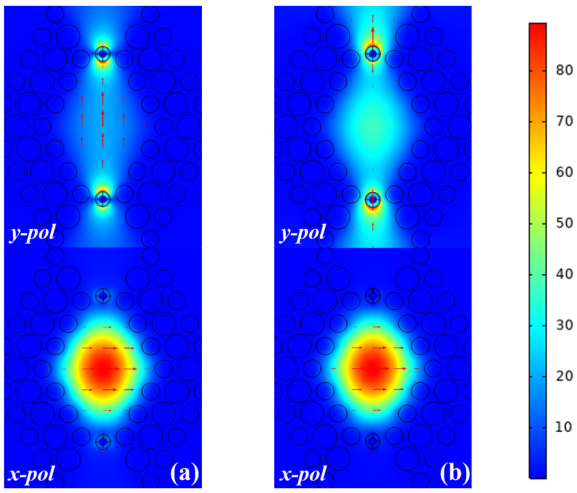

Fig. 3. The electromagnetic field distribution diagram of (a) y-pol and x-pol core mode at wavelength of 1519 nm; (b) y-pol and x-pol core mode at wavelength of 1664 nm.

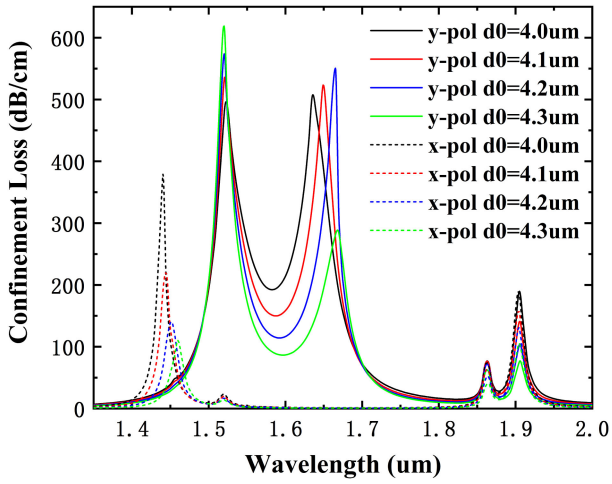

Fig. 4. The confinement loss curve with different d_0 and polarization states.

that resonance peak corresponding to the point where Re(neff) of SPP mode intersects with y-pol mode, and phase mutation of y-pol mode occurs. The value of y-pol loss peak 1 to peak 2 is 573.33 and 543.21 dB/cm, respectively, while the loss of x-pol mode is 16.97 and 0.98 dB/cm. Due to the strengthening effect to SPR of monocrystalline silicon, the x-pol SPP mode is also excited. It can be observed from the black solid line representing the loss of x-pol in the loss curve, the Re(neff) of the first-order SPP mode intersect with x-pol core mode at wavelength of 1452 nm and cause a phase mutation. In addition, there are two small resonant peaks of peak 3 and peak 4 appear at the longer wavelength. The numerical result reveals that the third-order and second-order SPP modes of y-pol direction are excited at the wavelength of 1862 and 1905 nm, respectively, at the same time the equivalent high-order SPP modes of x-pol direction are also excited at wavelength of 1863 and 1904 nm. The appearance of the synchronously identical high-order SPP modes at both y-pol and x-pol direction illustrate that the SPR occurs to the same extent in x-pol and y-pol direction, of which the formant peaks are very similar in amplitude and wavelength which resulting in no significant difference in the energy loss of different polarization direction.

Fig. 3 shows the electric field distribution diagrams of y-pol and x-pol mode at wavelength of 1519 and 1664 nm. Results show that the light of x-pol is well confined to central part while the light of y-pol direction couples with plasmon on gold contact surface to form a resonance so that the energy is absorbed and leaks to the outer cladding through the leakage channel. Furthermore, the confinement loss of y-pol direction mode at 1519 nm wavelength reaches a maximum value of 573.33 dB/cm. There is a difference between the resonance point of x-pol and y-pol mode, and there is no x-pol direction resonance when y-pol loss reaches peak1 and peak2. Therefore, the two main adjacent resonance peaks of y-pol bring extremely high extinction ratio within the operating bandwidth, improve the polarization performance, and achieved our design expectations.

According to the numerical results of original model, we adjusted and analyzed the structural parameters that can affect the polarization performance. The influence of the change of structural parameter on the shift of resonance wavelength, the change of CL of different polarization directions and the polarization extinction ratio are studied. It provides a theoretical basis for the design of the subsequent tunable PCF polarization filter.

It can be deduced from previous studies that the generation of surface plasmon resonance is significantly related to the incident angle and the intensity of incident light, and the Re(neff) of the contact surface. We change the distance d_0 of the gold wires used to initiate SPR from the core center to study the influence on the filter characteristics. As shown in Fig. 4, with the distance increase from 4.0 to 4.3 μm, the second resonance position is obviously red-shift. And the first resonance peak in y-pol direction increases and hit the maximum value at $d_0 = 4.3$ μm with the loss of 618.83 dB/cm at the 1515 nm wavelength. It is noticeable that the loss value of second peak goes down to 281.32 dB/cm at 1679 nm wavelength instead of further increase. Results reveal that as the incident angle shift with distance varies between gold wires and the core center, the phase matching conditions of y-pol mode and SPP mode are altered, the energy transfer from core mode to gold reduced accordingly. Based on the same principle, the resonance intensity of x-pol direction is enhanced when distance decreased from 4.3 to 4.0 μm and CL augment with the wavelength blue-shifting. In addition, other resonance points at y-pol direction are not sensitive to the changes of d_0, variation of the resonance point and confinement loss are slightly.

The influence of the first and the third layers air holes on the filter performance is reflected in Fig. 5. With the diameter of d_1 change from 0.9 to 1.2 μm, both of the first and second peaks of y-pol mode losses are blue-shifted, the loss peaks appear a trend of first increasing and then decreasing as the diameter d_1 largens. The first peak and second peak reach maximum loss value 593.41 and 543.21 dB/cm when d_1=1.1 μm and d_1=1 μm, respectively. For the second peak, the loss rises from 513 to 550.68 dB/cm,

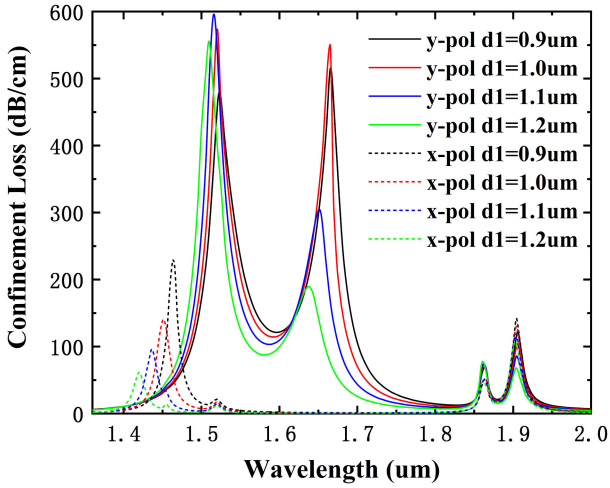

Fig. 5. The confinement loss curve with different d_1 and polarization states.

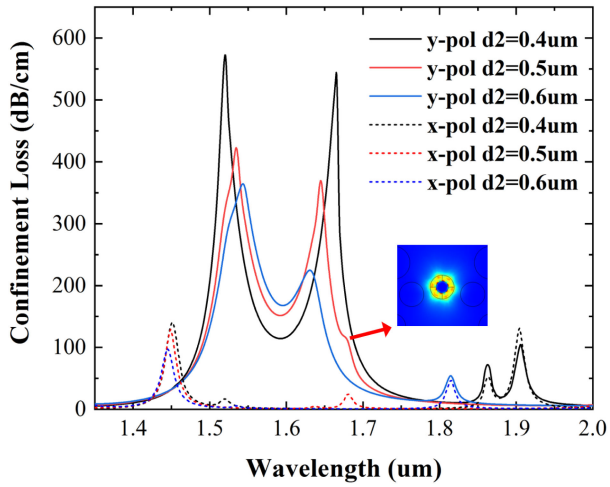

Fig. 6. The confinement loss curve with different d_2 and polarization states of x-pol and y-pol. When $d_2 = 0.5$ μm a resonant peak is observed at 1679 nm, and the electromagnetic field distribution profile shows a phase mutation in the y-polarization direction and a third-order SPP mode is excited.

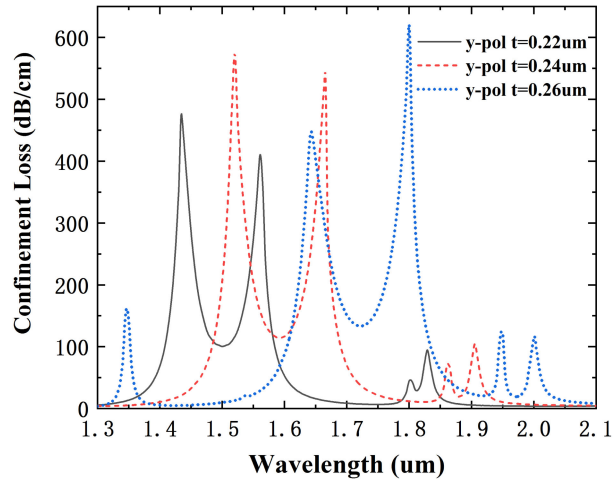

Fig. 7. The confinement loss curve of y-pol direction with different t. The remaining parameters are $d_0 = 4.2$ μm,$d_1 = 1$ μm, $d_2 = 0.4$ μm, $d_3 = 1.36$ μm.

and then there was a sharp drop in the loss value from 303.01 to 187.6 dB/cm. Obviously, large diameter air hole can better limit light to the core area, but because of more light is coupled with the plasma on the surface of gold wires, the loss reaches a maximum when d_1=1 μm.

Compared with aluminum and silver, gold exhibits more stable chemical properties, and appears a higher and sharper resonant peak. Therefore, gold is usually used as a responsive material in the research of SPR-PCF. The property of different diameter of introduced gold wires are analyzed. The loss curve can be seen from Fig. 6, as the diameter of gold wires increase, the values of the two resonant peaks decrease sharply, the loss values of first resonant peak are 573.33, 422.10, 359.27 dB/cm with d_2 of 0.4, 0.5 and 0.6 μm, respectively, and the resonant wavelength is redshift. For the second resonant peak, the loss values decrease from 543.21 to 357.01 dB/cm, and reach a minimum value of 225.38 dB/cm when d_2=0.6 μm, at the same time the resonant wavelength is blueshift. This phenomenon is consistent with previous studies [15], one theory explains that the thicker metals have higher damping loss, the evanescent waves penetration towards the metal weaken, and the presence of surface plasmons on the sensing medium is vanished dramatically, resulting in a decrease in sensing performance. Which is worth noting that a small resonant peak is generated at 1679 nm when d_2=0.5 μm, and the electromagnetic field distribution result show that a third-order SPP mode appears in the y-pol direction, as shown in the Fig. 6, however, the rapid attenuation of the higher-order mode allows resonance to last only a short wavelength. Based on the above results, in order to obtain better polarization performance, the gold wire diameter was optimized to 0.4 μm in this study.

As a major research focus in this study, the introduction of the monocrystalline silicon layer has an extremely important impact on the performance of the designed polarization filter. Fig. 7 shows the CL curve of different layer thickness of y-pol direction. It can be seen as the t thickening increasing, the resonance peak shifts towards the long wavelength direction. The two main resonance peaks have varying degrees of response, the first peak rises and reaches the maximum at thickness of 0.24 μm, and the second loss peak has a significant rise that the CL are 404.01, 543.21, 615.81 dB/cm with the thickness t of 0.22, 0.24, 0.26 μm. The thickness of the monocrystalline silicon layer changes the conditions of phase mutation, and cause the fluctuate in the amplitude of two resonant peaks. Compared with other parameters, layer thickness mainly affects the wavelength shift of resonance. Based on the above research, the performance of filter can be improved by optimizing the parameters of monocrystalline silicon layer to achieve the design expectations.

In addition, the ER of proposed PCF filter has been analyzed. As an important evaluation indicator for filter performance, the ER can be characterized by the following formula:

$$ER = 20lg\{exp[(\alpha_2 - \alpha_1)L]\} \tag{4}$$

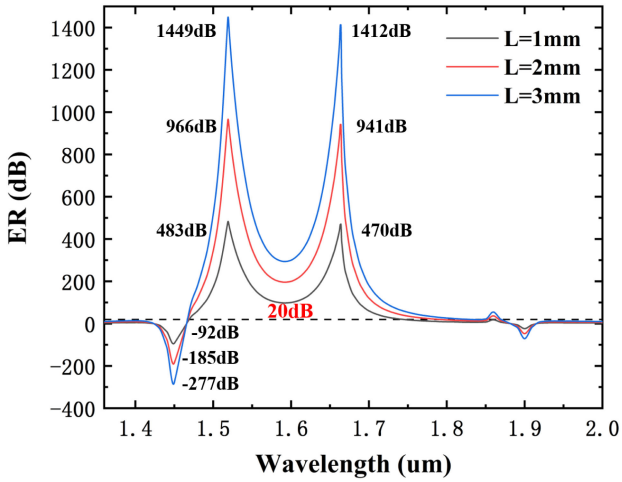

Fig. 8. The ER curve of the original structure parameters with fiber length of 1, 2, 3 mm.

TABLE II
COMPARISON WITH REPORTED PCF POLARIZATION FILTERS

References	Resonance wavelength(μm)	maxER /(dB)	BW /(nm)	Fiber length(mm)
gold layer[3]	1.5	326	300	1
gold layer[17]	1.55	326.7	480	1
uniformly hole[18]	1.55	\	120	1
This work	1.52, 1.66	1449	405	3

where α_2 and α_1 represent the loss of y-pol and x-pol mode, respectively, and L represents the fiber length. A conclusion can be found that ER has a linear relationship with the fiber length. As shown in Fig. 8, the main bandwidth of original structure with ER better than 20 dB can reach 405 nm, and two peaks value of ER are 1449 and 1412 dB when fiber length is 3 mm. Furthermore, due to the high loss caused by the phase coupling of x-pol mode at 1450 nm wavelength, a reverse filter channel is obtained with bandwidth of 38 nm. The proposed PCF filter achieves an extremely high ER within the operating bandwidth of 405 nm which would have great practical value in micro-nano optical integrated system.

The proposed and reported PCF filters are listed in Table II. Compared with the previous work, the filter proposed in this work has a higher polarization extinction ratio when the fiber length is only 3 mm, and the working bandwidth is also maintained at a high level.

The fabrication tolerances analysis is of great importance. By changing 5% based on the value of optimized structure parameters to analyze the characteristics of filter. It can be seen from Table III that the change of air hole parameters d_1 and d_3 and gold wire diameter d_2 can barely impact filtering performance. When the thickness of silicon layer t increases by 5%, the resonance wavelength shift from 1520 and 1660 nm to 1582 and 1736 nm, and the loss values reach 474 and 576 dB/cm which is also much larger than x-pol. In this case, great separation can be achieved in x and y direction and the proposed PCF has good adaptability to fabrication tolerance.

TABLE III
FABRICATION TOLERANCE OF PROPOSED PCF FILTER

Parameter	The fabrication tolerance analysis	Resonance wavelength of y-pol(nm)	CL of y-pol /(dB/cm)
d_1, d_3	+5%	1519, 1659	581.5, 539.7
	-5%	1520, 1665	562.2, 439.3
t	+5%	1582, 1736	474, 576
	-5%	1453, 1590	476, 462.8
d_2	+5%	1520, 1660	480, 491
	-5%	1515, 1666	498, 554

IV. CONCLUSION

In this research, via the innovative introduction of monocrystalline silicon coating, the CL in y-pol direction is enhanced and two adjacent resonance peaks are excited. Numerical analysis shows that the CL of y-pol reach 573.33 and 543.21 dB/cm, while the loss of x-pol is only 16.97 and 0.98 dB/cm. The maximum ER comes up to 1449 and 1412 dB with fiber length of 3 mm, and the filter bandwidth reaches 405 nm which includes the entire communication band. In addition, the influence of fiber structure parameters is quantitatively analyzed, results show that the thickness of monocrystalline silicon has a significant effect on the wavelength shift of resonance peak, which means that the filter can be applied to different wavebands by adjusting the layer thickness. Therefore, the proposed PCF filter has excellent polarization performance and has potential application value in the fields of optical communication, integrated optical system and optical sensing.

REFERENCES

[1] Y. Wang, S. Li, J. Li, Y. Guo, and M. Wang, "Novel external gold-coated side-leakage photonic crystal fiber for tunable broadband polarization filter," *J. Lightw. Technol.*, vol. 39, no. 6, pp. 1791–1799, Mar. 2021.
[2] J. Wu, S. Li, X. Jing, D. Chao, and Y. Wang, "Elliptical photonic crystal fiber polarization filter combined with surface plasmon resonance," *IEEE Photon. Technol. Lett.*, vol. 30, no. 15, pp. 1368–1371, Aug. 2018.
[3] M. Chang, B. Li, N. Chen, X. Lu, X. Zhang, and J. Xu, "A compact and broadband photonic crystal fiber polarization filter based on a plasmonic resonant thin gold film," *IEEE Photon. J.*, vol. 11, no. 2, 2020, Art. no. 7202312.
[4] K. Ahmed, M. Reyad-Ul-Ferdous, M. N. Hossen, B. K. Paul, and P. Yupapin, "Low insertion loss and high extinction ratio analysis of a new surface plasmon resonance based photonic crystal fiber filter," *Optik*, vol. 194, 2019, Art. no. 163069.
[5] B. K. Paul et al., "Design and analysis of slotted core photonic crystal fiber for gas sensing application," *Results Phys.*, vol. 11, pp. 643–650, 2018.
[6] D. Lu, X. Fang, X. Li, and Z. Li, "Single-polarization single-mode photonic crystal fibers with uniformly sized air holes," *J. Lightw. Technol.*, vol. 39, no. 99, pp. 620–626, Jan. 2021.
[7] Y. L. Yu, H. Kishikawa, S. K. Liaw, M. Adiya, and N. Goto, "Broadband silicon core photonics crystal fiber polarization filter based on surface plasmon resonance effect," *Opt. Commun.*, vol. 482, 2021, Art. no. 126587.
[8] C, A. Pfeiffer, E. N. Economou, and K. L. Ngai, "Surface polaritons in a circularly cylindrical interface: Surface plasmons," *Phys. Rev. B*, vol. 10, pp. 8–15, 1974.
[9] M. A. Schmidt, L. Sempere, H. K. Tyagi, C. G. Poulton, and P. Russell, "Waveguiding and plasmon resonances in two-dimensional photonic lattices of gold and silver nanowires," *Phys. Rev. B*, vol. 77, no. 3, 2008, Art. no. 033417.
[10] B. K. Paul, F. Ahmed, M. G. Moctader, K. Ahmed, and D. Vigneswaran, "Silicon nano crystal filled photonic crystal fiber for high nonlinearity," *Opt. Mater.*, vol. 84, no. 17, pp. 545–594, 2018.

[11] M. R. Hasan et al., "Spiral photonic crystal fiber-based dual-polarized surface plasmon resonance biosensor," *IEEE Sensors J.*, vol. 18, no. 1, pp. 133–140, Jan. 2018.

[12] B. Shuai, L. Xia, Y. Zhang, and D. Liu, "A multi-core holey fiber based plasmonic sensor with large detection range and high linearity," *Opt. Exp.*, vol. 20, no. 6, pp. 5974–5986, 2012.

[13] C. D. Salzberg and J. J. Villa, "Infrared refractive indexes of silicon germanium and modified selenium glass," *J. Opt. Soc. Amer.*, vol. 47, no. 3, pp. 244–246, 1957.

[14] J. N. Dash and R. Jha, "On the performance of graphene-based D-shaped photonic crystal fibre biosensor using surface plasmon resonance," *Plasmonics*, vol. 10, no. 5, pp. 1123–1131, 2015.

[15] H. Chen et al., "Filtering characteristics and applications of photonic crystal fibers being selectively infiltrated with one aluminum rod," *J. Lightw. Technol.*, vol. 34, no. 21, pp. 4972–4980, 2016.

[16] A. A. Rifat, R. Ahmed, G. A. Mahdiraji, and F. R. M. Adikan, "Highly sensitive D-shaped photonic crystal fiber based plasmonic biosensor in visible to near-IR," *IEEE Sensors J.*, vol. 17, no. 9, pp. 2776–2783, May 2017.

[17] Y. Guo, J. Li, S. Li, S. Zhang, and Y. Liu, "Broadband single-polarization filter of D-shaped photonic crystal fiber with a micro-opening based on surface plasmon resonance," *Appl. Opt.*, vol. 57, no. 27, pp. 8016–8022, 2018.

[18] D. Lu, X. Fang, X. Li, and Z. Li, "Single-polarization single-mode photonic crystal fibers with uniformly sized air holes," *J. Lightw. Technol.*, vol. 39, no. 2, pp. 620–626, Jan. 2021.